Supplementary Information

eMethods. Participants, phenotyping, assessment of balance and covariates in MVP, genotyping and imputation, relatedness, calculation of principal components (PCs), GWAS in MVP, estimating SNP-based heritability (h^2_{SNP}), colocalization of eQTL with GWAS results, replication in European meta-analysis from Iceland/Finland/UKB/US, CC-GWAS, fine-mapping, functional mapping and annotation, gene-based and gene set analysis with MAGMA, genetic correlations of tinnitus with other cochlear disorders, pheWAS of other disorders.

Table e1. Participants removed for in-patient and out-patient diagnoses.

Table e2. Linkage Disequilibrium Score on cochlear disorders and replication cohort.

Table e3. Case-case GWAS EU Balance compared to replication cohort.

Table e4. Gene-tissue expression in 53 tissues, including chromatin interactions.

Table e5. Functional analysis of lead SNPs.

Table e6. PheWAS results for lead SNPs.

Figure e1. Quantile-quantile plot of expected versus observed -log10 *P*-values for a genome-wide association study (GWAS) of chronic imbalance.

Figure e2. Regional association plots (Locus zoom) of top hit rs12779865 in trans-ancestry GWAS with annotations regarding pathogenicity, transcription-factor binding sites, and chromatin state.

Figure e3. Regional association plots (Locus zoom) of top hit rs72631329 in the trans-ancestry GWAS with annotations regarding pathogenicity, transcription-factor binding sites, and chromatin state.

Figure e4. Regional association plots (Locus zoom) of top hit rs10713223 in trans-ancestry GWAS with annotations regarding pathogenicity, transcription-factor binding sites, and chromatin state.

Figure e5. Regional association plots (Locus zoom) of top hit rs200689072 in trans-ancestry GWAS with annotations regarding pathogenicity, transcription-factor binding sites, and chromatin state.

Figure e6. Regional association plots (Locus zoom) of top hit rs10828248 in European (EU) GWAS with annotations regarding pathogenicity, transcription-factor binding sites, and chromatin state.

Figure e7. Regional association plots (Locus zoom) of top hit rs7221651 in EU GWAS with annotations regarding pathogenicity, transcription-factor binding sites, and chromatin state.

Figure e8. Regional association plots (Locus zoom) of top hit rs4791046 in EU >= age 50 GWAS with annotations regarding pathogenicity, transcription-factor binding sites, and chromatin state.

Figure e9. Regional association plots (Locus zoom) of top hit rs71717606 in Hispanic (LA) GWAS with annotations regarding pathogenicity, transcription-factor binding sites, and chromatin state.

Figure e10. Fine-mapping plots.

Figure e11. PheWAS on lead SNPs with annotation of top hits.

Supplementary Methods:

Participants

The Million Veteran Program (MVP) cohort consists of 819,307 participants (version 20_1) recruited since 2011. After written informed consent, participants filled out two basic health question surveys and had bloods drawn for genotyping. Information including ICD diagnostic codes, questionnaires, VA and active-duty health records are all linked to de-identified ID#'s. Participants filled out lifestyle questionnaires in regard to demographics, lifestyles, work, military experience, and self-reported health conditions. All participants provided written informed consent to participate.

Phenotyping - Assessment of chronic imbalance and other variables in MVP

Balance was assessed by ICD. Phenotype consisted of two diagnoses that contained dizziness, imbalance, or vertigo, at least 180 days apart, indicating chronicity. ICD's included were identified within the Veteran's Administration Informatics and Computing Infrastructure (VINCI) space via SQL tables of diagnoses and descriptions.

Excluded ICD's both ICD9 and ICD10 were the following: 332.1, 334.x ataxias, 342.x hemiplegias, 386 Meniere's disease, 438.84 ataxia 780.2 syncope, 966.4 poisoning, E855.0 accidental overdose, E936.4 Parkinson's medications, G20 Parkinson's Disease, G21.x Secondary Parkinson's, G32.81 cerebellar ataxia, G60.2 neuropathy associated with hereditary ataxia, G80.x cerebral palsy and paralytic syndromes, G90.01 familial dysautonomia, G81.x hemiplegia, H81.01 Meniere's disease, H82.1 benign positional paroxysmal vertigo, H81.2 vestibular neuronitis, I69.x ataxia following subarachnoid hemorrhage, R27.0 ataxia, R55 syncope and collapse, T42.8x1A poisoning by Parkinson's medication, T67.1xxA heat syncope, T75.22xA external causes of spasticity, and R55 syncope.

Since a traumatic brain injury (TBI) can lead to vertigo, if the subject had a positive ICD for dizziness or vertigo AND had evidence of TBI, they were excluded. These diagnoses included S06.2x0A traumatic brain injury, S06.2x diffuse brain injury, S06.x intracranial injury, and V15.52 history of TBI.

Controls were those no evidence of imbalance in the electronic health record (EHR).

Here is a list of exclusions (note some participants fit into several categories):

- East and West Asians: 6,326
- < 180 days between diagnoses: 121,745
- Diagnoses:
  A. Acute diagnoses, such as Meniere's Disease, benign paroxysmal positional vertigo, vestibular neuronitis, viral labyrinthitis – 26,353
  B. Ataxias, including Parkinson's, cerebral ataxia, hereditary ataxias, following arachnoid hemorrhage – 27,768
  C. Cerebral palsy – 206
  D. Hemiplegia, cerebrovascular accident, stroke – 35,551
  E. Poisoning and overdose – 38,005
  F. Syncope, including heat syncope – 115,709
  G. Traumatic brain injury, intracranial injury, history of TBI – 54,722

Genotyping and imputation

Analyses were based on the version 3 release of the MVP unimputed genetic dataset and version 3 release of the MVP imputed genetic dataset. Details of genotyping, quality control, and imputation of the MVP have been previously reported.[19] In brief, blood samples were gathered from subjects after written consent had been obtained, beginning in 2011. The Advanced Marker QC Pipeline excluded probeset calls from batches that fail advanced QC tests, as described previously (Hunter-Zinck, et al, 2020). Samples are stored at MAVERIC, VA Boston, MA. DNA was extracted and sent for genotyping at the Affymetrix Research Services Laboratory. Subjects were genotyped on either the Affymetrix Axiom or UK BiLEVE Axiom arrays, with approximately 4,700 samples per batch. Genotype calling was performed using a custom pipeline designed for biobank scale data. Routine quality control procedures were performed at each step of genotype extraction and calling. Quality control of marker genotypes included tests for batch and plate effects, deviations from Hardy-Weinberg equilibrium based on exact tests, sex effects, array effects, and discordance among technical replicates. Based on markers passing QC, subjects were removed for >2% missing genotype rate, discrepancy between self-reported sex and genetically determined sex, or excessive heterozygosity. Phasing was performed using SHAPEIT3 in partially overlapping chunks of 15,000 markers, with the 1000 Genomes Phase 3 dataset used as a reference panel. Chunks were merged using hapfuse. Data was imputed using IMPUTE4, using the combination of the 1000 Genomes Phase 3, UK10K, and Haplotype Reference Consortium panels, where the latter was preferentially used as the imputation reference.

Relatedness

Although REGENIE compensates for relatedness, nevertheless, related individuals were removed. Relatedness was estimated using KING. For analyses of unrelated subjects, from each pair with an estimated kinship coefficient > 0.0442 (3rd degree or closer), the individual with higher tinnitus symptoms was retained, and for pairs with identical symptoms, one was chosen at random.

Calculation of principal components (PCs) to address population stratification

SNPs were excluded that had a MAF < 5%, HWE p > $1x10^{-3}$, call rate < 98%, were ambiguous (A/T, G/C), located in the MHC region (chr6, 25-35 MB) or chromosome 8 inversion (chr8, 7-13 MB). SNPs were pairwise LD-pruned ($r^2 > 0.2$) and a random set of ~100K markers was used for each subset to calculate PCs based on the smartPCA algorithm in EIGENSTRAT.

GWAS in MVP

REGENIE was run using a 2-step process as described (Mbatchou et al., 2021). REGENIE is a machine-learning method using a mixed-model-based approach that uses ridge regression to combine a set of correlated predictors based on unimputed SNPs to fit a model in Step 1. Since this is a binary trait, logistic regression with Firth correction was used. In Step 2, imputed variants based on BGENS data in MVP are tested for association conditional on the

predictions of Step 1, using the leave-one-chromosome-out scheme. Chunks consist of 219 MB for Rel4. Covariates include 10 principal components, age, and sex.

Summary statistics were filtered to MAF ≥ 1% and INFO score ≥ 0.6. Quantile-quantile (QQ) plots of expected versus observed -$\log_{10}$ *P*-values included genotyped and imputed SNPs at MAF ≥ 1%. The proportion of inflation of test statistics due to the actual polygenic signal (rather than other causes such as population stratification) was estimated as 1 - (1 - LDSC intercept - 1)/(mean observed chi-square - 1), using LD-score regression.[8] For primary analyses, genome-wide significance was declared at $P < 5 \times 10^{-8}$. Regional association plots were generated using LocusZoom with 400KB windows around the index variant with LD patterns calculated based on 1KGP EUR, AMR, or multiple reference populations for transancestry analysis.[9]

Replication in Iceland/Finland/UK/US cohort

Methods of the replicating GWAS are explained in detail in the original paper. Briefly, the meta-analysis consisted of cohorts in Iceland (30,802 cases and 278,502 controls), the UK (9715 cases and 421,332 controls), the US (1888 cases and 24,961 controls), and Finland (5667 cases and 169,746 controls). Phenotype was defined as an ICD of vertigo, including ICD9 386.x and ICD10 of H81.xx.

For GWAS, a logistic regression assuming an additive model was tested using deCODE. LD score regression accounted for distribution inflation secondary to cryptic relatedness and population stratification. A fixed effect inverse variance method based on effect estimates and standard errors was used, where study groups were assumed to have a common odds ratio but allowed to have different population frequencies for alleles. Total number of variants were 62,056,310 spread over the four populations. GWAS significance was calculated using a weighted Bonferroni adjustment controlling for the family-wise error rate. Variants had been mapped to NCBI Build38, and for this study, required lift-over to GrCh37. In a random-effects method, a likelihood ratio test was performed on GWAS associations to test heterogeneity.

Estimating SNP-based heritability *(h^2_{SNP})*

SNP-based heritability estimates (h^2_{SNP}) were calculated using LDSC on GWAS summary data. Estimates were calculated for each version of the tinnitus phenotype, and statistical models including covariates age and hearing difficulties, and for men and women separately. Unconstrained regression intercepts were used to account for potential inclusion of related subjects and residual population stratification, and precomputed LD-scores from 1KGP EUR populations were used. To test for sex-specific heritability, a z-test was performed on the difference of the effect estimates from sex-stratified analyses.

Cohen's D

Cohen's D was calculated to ascertain whether there was a difference in effect size between the European cohort and those over 50 years of age. Comparisons were computed for the lead SNP effect sizes in chromosomes 10 and 17, using beta for effect sizes, and converting standard error to standard deviation corrected for sample size in each cohort.

CC-GWAS between Ice/Fin/UKB/US cohorts

Case-case GWAS was performed to test for differences between SNPs of disorders. Input consists of effect sizes, effective N's for cases and controls, P-values, population statistics and heritability for the disorders, and overlap between the two cohorts. For significant SNPS (P-

value = 5.0e-10), output included statistically significant effect sizes reflecting direction and magnitude of effect, discards false positives, and measures genetic distance between the two disorders (Peyrot, 2021).

Fine-mapping with sum of single effects model.

An interval of 2.5 million base-pairs surrounding each significant locus was identified. This range was then downloaded from EnSembl in Data Slicer using these chromosome positions in GrCh38 and ancestries to match our lead SNPs from the 1000 genome. For example, since significant SNPs for the European cohort were identified in chromosomes 10 and 17, the ld matrix was fashioned from 1000 genomes of CEU individuals. Plink was then used to convert the .vcf file to plink binary, then linkage disequilibrium matrices were fashioned for use in susieR.

A fitted regression with summary statistics was fashioned for each significant locus, which created "credible sets" of potentially causal variants, based on posterior probability of 0.95, with 100 iterations and refinement of the model. Increasing the iterations did not improve the model.

Functional mapping and annotation

We used Functional Mapping and Annotation of genetic associations (FUMA) v1.3.5 (http://fuma.ctglab.nl/) to annotate GWAS data and obtain functional characterization of risk loci.[10] Annotations are based on human genome assembly GRCh37 (hg19). FUMA was used with default settings unless stated otherwise. The SNP2Gene module was used to define independent genomic risk loci and variants in LD with lead SNPs ($r^2 > 0.6$, calculated using ancestry appropriate 1KGP reference genotypes). SNPs in risk loci were mapped to protein coding genes with a 10kb window.

Functional consequences of SNPs were obtained by mapping the SNPs on their chromosomal position and reference alleles to databases containing known functional annotations, including ANNOVAR, Combined Annotation Dependent Depletion (CADD), RegulomeDB (RDB), and chromatin states in brain tissues/cell types. Next eQTL mapping was performed on significant (FDR < 0.05) SNP-gene pairs, mapping to GTEx v7 brain tissue, RNAseq data from the CommonMind Consortium and the BRAINEAC database. Chromatin interaction mapping was performed using built-in chromatin interaction data from the dorsolateral prefrontal cortex, hippocampus and neuronal progenitor cell line and adult and fetal cortex tissue. An FDR of $< 1x10^{-5}$ defined significant interactions, based on previous recommendations, modified to account for the differences in cell lines used here.

Gene-based and gene set analysis with MAGMA

Gene-based analysis was performed with the FUMA implementation of MAGMA.[11] SNPs were mapped to 18,222 protein coding genes. For each gene, its association with tinnitus was determined as the weighted mean squared test statistic of SNPs mapped to the gene, where LD patterns were calculated using ancestry appropriate 1KGP EUR reference genotypes. Significance of genes was set at a Bonferroni-corrected threshold of *P* value = 0.05/18,222 = 2.7 x 10^{-6}.

To see if specific biological pathways were implicated in tinnitus, gene-based test statistics were used to perform a competitive set-based analysis of 10,894 pre-defined curated gene sets and GO terms obtained from MsigDB using MAGMA. Significance of pathways was set at a Bonferroni-corrected threshold of $P = 0.05/10,894 = 4.6 \times 10^{-6}$. To test if tissue-specific

gene expression was associated with tinnitus, gene set-based analysis was also used with expression data from GTEx v7 RNA-seq and BrainSpan RNA-seq, where the expression of genes within specific tissues were used to define the gene properties used in the gene-set analysis model.

Table e1. Diagnoses Removed from Phenotype

Description	In_patient	Out_patient	Total
Benign Paroxysmal Positional Vertigo	3,506	40,126	41,233
Meniere's Disease	947	5,243	5,446
Vestibular Neuronitis	2,812	25,389	26,353
Cerebral ataxia, Parkinson, hereditary ataxia	8,521	25,185	27,768
Cerebral Palsy	45	174	219
Hemiplegia, stroke	16,461	28,412	35,551
Poisoning and overdose	16,838	28,367	38,005
TBI, diffuse brain injury, intracranial injury	12,007	50,775	54,722
Syncope, including heat and orthostatic hypotension	32,994	110,125	115,709
TOTALS (may overlap)	94,131	313,796	345,006

Table e2. Linkage disequilibrium scores on cochlear disorders and replication cohort.

p1	p2	rg	se	Z-score	P value	h2_p1_liab	h2_p1_SE	h2_p2_liab	h2_p2_se	h2_int	h2_int_se	gcov_int	gcov_int_se
balance	**Skuladottir**	0.6721	0.0734	9.1569	5.3433e-20	0.0469	0.0059	0.0666	0.0074	1.0053	0.0076	0.0051	0.0052
balance	**tinnitus**	0.2025	0.0833	2.4304	0.0151	0.0462	0.0066	0.1026	0.0066	1.0116	0.0074	0.0028	0.0059
balance	**hearing**	0.3148	0.0481	6.5495	5.7721e-11	0.0461	0.0059	0.1199	0.0006	1.0273	0.0094	0.0002	0.0053
tinnitus	**hearing**	0.5184	0.0309	16.7584	4.9136e-63	0.1071	0.0067	0.1193	0.0058	1.0282	0.0081	0.1544	0.0054
Skuladottir	**tinnitus**	0.1925	0.049	3.9242	8.7001e-05	0.067	0.0072	0.1066	0.0068	1.0098	0.0073	0.0283	0.0048
Skuladottir	**hearing**	0.1859	0.0491	3.7821	0.0002	0.067	0.0072	0.1208	0.006	1.0266	0.0087	0.0183	0.0052
balance	**balance>49**	0.9787	0.0063	154.2505	0.0	0.0459	0.0058	0.0482	0.007	1.0217	0.0075	0.9827	0.0074
EU Bal_90	**EU Bal_180**	1.0015	0.0035	288.075	0.0	0.0172	0.0024	.0172	.0024	1.0263	0.0100	0.9886	0.0098

Abbreviations: pl, phenotype 1; p2, phenotype 2; rg, genomic correlation; se, standard error; h2, SNP inheritability on the liability scale; int, intercept, gcov, genetic covariance; EU Bal_90 European cohort for 2 diagnoses of dizziness greater than 90 days apart; EU Bal_180 European cohort for 2 diagnoses greater than 180 days apart.

Balance study – Trans-ancestry GWAS from Million Veterans Program

Tinnitus study – European GWAS performed in UK Biobank (Clifford, et. al, 2020)

Hearing study – European GWAS performed in UK Biobank (Wells, et al, 2019)

Skuladottir, et al. – European meta-analysis GWAS on Iceland/Finland/UKBiobank/US for diagnosis of vertigo (Skuladottir, et al., 2021)

Table e3. Case-case European Balance GWAS compared to Replication Cohort[1]

SNP	CHR	BP	EA	NEA	OLS_beta	OLS_se	OLS_pval	Exact_beta	Exact_se	Exact_pval	CCGWAS_signif
rs403983	19	23484776	G	A	-2.97E-03	5.27E-04	1.81E-08	-1.82E-02	3.22E-03	1.55E-08	1
rs17473980	19	23512665	G	T	-5.24E-03	5.27E-04	2.82E-23	-3.22E-02	3.22E-03	1.72E-23	1
rs11667562	19	23513267	T	G	-4.98E-03	5.27E-04	3.80E-21	-3.06E-02	3.22E-03	2.55E-21	1
rs12151189	19	23517735	C	T	-4.97E-03	5.27E-04	4.13E-21	-3.05E-02	3.22E-03	2.78E-21	1
rs35367868	19	23527117	C	T	-4.99E-03	5.27E-04	2.90E-21	-3.07E-02	3.22E-03	1.94E-21	1
rs295390	19	23528350	T	C	-4.91E-03	5.27E-04	1.31E-20	-3.02E-02	3.22E-03	8.40E-21	1
rs1020075	19	23540217	T	C	-4.97E-03	5.27E-04	4.09E-21	-3.05E-02	3.22E-03	2.75E-21	1
rs35804934	19	23557070	A	G	-3.24E-03	5.27E-04	8.51E-10	-1.98E-02	3.22E-03	8.67E-10	1
rs641702	19	23593010	G	T	-5.11E-03	5.27E-04	3.38E-22	-3.14E-02	3.22E-03	2.23E-22	1
rs147995216	19	23601870	G	A	-5.08E-03	5.27E-04	5.49E-22	-3.12E-02	3.22E-03	3.61E-22	1
rs12983355	19	23607974	G	T	-4.40E-03	5.27E-04	6.75E-17	-2.70E-02	3.22E-03	5.05E-17	1
rs12985969	19	23611666	A	C	-5.08E-03	5.27E-04	6.04E-22	-3.12E-02	3.22E-03	4.00E-22	1
rs2219838	19	23634712	C	T	-3.05E-03	5.27E-04	7.62E-09	-1.86E-02	3.22E-03	7.63E-09	1
rs10413718	19	23655398	T	G	-4.06E-03	5.27E-04	1.34E-14	-2.49E-02	3.22E-03	1.02E-14	1
rs8108305	19	23665224	T	C	-4.06E-03	5.27E-04	1.39E-14	-2.49E-02	3.22E-03	1.06E-14	1
rs10420240	19	23670982	G	A	-3.95E-03	5.27E-04	6.40E-14	-2.43E-02	3.22E-03	5.03E-14	1

Abbr: SNP, single nucleotide polymorphism; CHR chromosome; EA, effect allele; NEA, non-effect allele; OLS ordinary least-squares; pval, P-value; se, standard error; CCGWAS signif, case-case genome-wide association study – a comparison of alleles at each SNP.

[1] Based on comparison of 7,600,837 overlapping SNPs between EU GWAS and Ice/UK/US/Fin replication.

Table e4. Gene-Tissue Expression in 53 tissues with addition of chromatin interactions.

VARIABLE	BETA	BETA_STD	SE	P
Brain_Cerebellar_Hemisphere	0.024937	0.050001	0.0062109	2.99E-05
Brain_Cerebellum	0.024979	0.049545	0.0063991	4.76E-05
Brain_Frontal_Cortex_BA9	0.019148	0.035243	0.0070027	0.0031278
Brain_Cortex	0.019399	0.03534	0.0072543	0.0037498
Pituitary	0.021851	0.040672	0.0091688	0.0085881
Brain_Anterior_cingulate_cor...	0.015181	0.026789	0.0073387	0.019299
Brain_Spinal_cord_cervical_c...	0.016329	0.029318	0.0088446	0.032442
Brain_Putamen_basal_ganglia	0.013628	0.023169	0.0080772	0.045788
Brain_Hippocampus	0.01341	0.022686	0.0081126	0.049181
Brain_Caudate_basal_ganglia	0.012384	0.021369	0.0080142	0.061152
Brain_Amygdala	0.010826	0.018424	0.0079675	0.087128
Brain_Nucleus_accumbens_basa...	0.01035	0.017938	0.0077289	0.090277
Brain_Hypothalamus	0.0095061	0.016342	0.0082465	0.12452
Brain_Substantia_nigra	0.0098406	0.016924	0.0087676	0.13086
Prostate	0.008112	0.015366	0.012212	0.25326
Whole_Blood	0.0029887	0.0054018	0.0057267	0.30088
Liver	0.0032138	0.0057853	0.0065339	0.31141
Small_Intestine_Terminal_Ile...	0.0048361	0.0088795	0.0098472	0.31168
Stomach	0.0058953	0.010698	0.012355	0.31663
Muscle_Skeletal	0.0030005	0.005676	0.0071178	0.33668
Ovary	0.00029856	0.00060469	0.0099363	0.48801
Heart_Left_Ventricle	-0.00099425	-0.0016592	0.0093169	0.54249
Bladder	-0.0031143	-0.0060624	0.013287	0.59266
Heart_Atrial_Appendage	-0.0030471	-0.0054671	0.0097693	0.62244
Pancreas	-0.002821	-0.004716	0.0086482	0.62786
Adrenal_Gland	-0.0038153	-0.007359	0.010246	0.64519
Cervix_Endocervix	-0.0054448	-0.010763	0.011856	0.67697
Cells_EBV-transformed_lympho...	-0.0023749	-0.0051821	0.0050178	0.682

Colon_Transverse	-0.0076424	-0.014033	0.011872	0.74012
Testis	-0.0037007	-0.006376	0.0056747	0.74284
Esophagus_Gastroesophageal_J...	-0.010153	-0.019969	0.013208	0.77896
Uterus	-0.0093772	-0.019085	0.011163	0.79954
Spleen	-0.0072687	-0.014393	0.0074528	0.83528
Cervix_Ectocervix	-0.01484	-0.02905	0.012377	0.88473
Lung	-0.011574	-0.022345	0.009339	0.89239
Esophagus_Muscularis	-0.015937	-0.031409	0.012793	0.89356
Artery_Tibial	-0.012876	-0.026489	0.010323	0.89385
Kidney_Medulla	-0.011939	-0.022052	0.0095334	0.89476
Fallopian_Tube	-0.015477	-0.029978	0.012199	0.89772
Colon_Sigmoid	-0.017027	-0.033275	0.012915	0.9063
Kidney_Cortex	-0.013487	-0.023676	0.0092842	0.92684
Skin_Sun_Exposed_Lower_leg	-0.012154	-0.023554	0.0078837	0.9384
Artery_Aorta	-0.016264	-0.033163	0.010519	0.93895
Skin_Not_Sun_Exposed_Suprapu...	-0.012257	-0.023611	0.0078599	0.94055
Minor_Salivary_Gland	-0.016657	-0.030963	0.009838	0.95478
Thyroid	-0.017333	-0.034282	0.0098778	0.96034
Nerve_Tibial	-0.01882	-0.037828	0.010344	0.96556
Cells_Cultured_fibroblasts	-0.014839	-0.03178	0.0066835	0.98679
Adipose_Subcutaneous	-0.024551	-0.048951	0.011017	0.98707
Vagina	-0.025374	-0.048454	0.011223	0.98811
Breast_Mammary_Tissue	-0.030297	-0.058188	0.012921	0.99048
Esophagus_Mucosa	-0.018348	-0.035437	0.0077716	0.99088
Adipose_Visceral_Omentum	-0.028133	-0.054587	0.011358	0.99337
Artery_Coronary	-0.030466	-0.060584	0.012208	0.99371

European GWAS in MVP. Significant p-value = 0.05/53 = 9.4 x 10^{-04}. MEAN_SAMPLE_SIZE = 54557. TOTAL_GENES = 17236

Table e5. Functional analysis of lead SNPs

Ancestry	Lead Variant	P-value	Risk Locus	# SNPS in LD > .6	Predicted Genes in Locus	SNPS in LD[a] CADD[b] > 12.37
Trans-ancestry	rs12779865	3.65E-08	10:21769994-22285371	91	SKIDA1, MLLT10, DNAJC1, CASC10	rs12770228
	rs72631329	7.61E-09	17:65814382-66098154	333	BPTF, C17orf58, KPNA2	rs12452511, rs1976053, rs75360723, rs75360723, rs4318247, + 5 more
	rs10713223	3.11E-08	19:23490203-23642411	89	ZNF91	rs428549, rs397756857, rs10585848
	rs200689072	2.43E-08	21:18512554-18548915	16	none	rs8134340
CEU	rs10828248	3.17E-08	10:21766969-22288132	145	SKIDA1; MLLT10; DNAJC1; CASC10	rs12256551, rs946711, rs12770228, rs66955492, rs11012786
	rs7221651	3.71E-10	17:65764164-66098154	404	BPTF, C17orf58, KPNA2	rs12452511, rs1976053, rs75360723, rs11656743, rs75868869, + 3 more
CEU > 50	rs10828248	1.49E-08	10:21766969-22288132	145	SKIDA1, MLLT10, DNAJC1, CASC10	rs12452511, rs1976053, rs75360723, rs75360723, rs4318247, + 5 more
	rs4791046	5.24E-09	17:65764164-66096529	351	BPTF, C17orf58, KPNA2	rs12452511, rs1976053, rs75360723, rs11656743, rs75868869, + 3 more
MXL	rs71717606	4.84E-10	6:117683821-117822159	169	GOPC, ROS1, DCBLD1	rs2229079, rs368013630, rs72951624, rs9489171, rs17079187, rs56115066

Abbreviations: SNPs, single nucleotide polymorphisms; LD linkage disequilibrium;, eQTL, expression quantitative trait locus; Hi-C, hybridization capture of chromatin interactions.

[a] When > 5 are in this category, only the top 5 are listed.

[b] CADD is an *in silico* prediction of variant pathogenicity. >12.37 is a suggested threshold for pathogenicity.

[c] RegulomeDBscore < 5 indicates increased possibility of regulatory element binding sites.

[d] Hi-C provides evidence for chromatin interaction.

Table e5. Functional analysis of lead SNPs (continued)

Ancestry	Lead Variant	RegulomeDB[c] < 5
Trans	rs12779865	rs12770228, rs12357321, rs11012726, rs11012732, rs10828252, … + 5
	rs72631329	rs3936134, rs12451721, rs7214119, rs62084208, rs115210018, + 27 more
	rs10713223	rs11882589, rs641702, rs603909, rs695017, rs586413, + 3 more
	rs200689072	none
CEU	rs10828248	rs946711, rs10828249, rs10828247, rs2807986, rs12251016, + 19 more
	rs7221651	rs3936134, rs12451721, rs7214119, rs62084208, rs12452511, + 36 more
CEU > 50	rs10828248	rs946711, rs10828249, rs10828247, rs2807986, rs12251016, + 19 more
	rs4791046	rs3936134, rs12451721, rs7214119, rs62084208, rs62084208, + 29 more
MXL	rs71717606	rs72965306, rs72965317, rs72969456, rs72959668, rs72959686, rs56741692, rs55977400, rs59267160, rs56115066

Table e5 (continued)

		eQTL (13 neural tissue/cell lines)	Hi-C[d] in tissue cell line datasets
Ancestry	**Lead Variant**	**GTEx/v8**	
Trans	rs12779865	CASC1 in cerebellum	SKIDA1 intrachromosomal adult cortex, COMMD3-BMI1 in hippocampus and dorsolateral prefrontal cortex, SPAG6 intrachromosomal in hippocampus, and DPFC
	rs72631329	KPNA2 Cerebellar hemisphere, amygdala, nucleus accumbens basal gangia; BPTF cerebellum, cerebellar hemisphere	
	rs10713223	none	none
	rs200689072	none	none
CEU	rs10828248	MLLT10 anterior cinguate cortex, CASC10 cerebellum	MLLT10 hippocampus, DNAJC1 dorsolateral prefrontal cortex, hippocampus
	rs7221651	KPNA2 caudate basal ganglia, amygdala, nucleus aNoneccumbens basal ganglia, BPTF cerebellum, cerebellar hemisphere	none
CEU > 50	rs10828248	MLLT10 anterior cinguate cortex, CASC10 cerebellum	MLLT10 hippocampus, DNAJC1 dorsolateral prefrontal cortex, hippocampus
	rs4791046	KPNA2 in anterior cingulate cortex, brain cortex; BPTF cerebellum, cerebellar hemisphere	
MXL	rs71717606	ROS1, GOPC, DCBLD1 in cortex, GOPC, DCBLD1 in frontal cortex	DCBLD1 intrachromosomal in hippocampus

Table e6. PheWAS results for lead SNPs.

Chr 6 rs72965321 Significant P-value 4.31e-04

PMID	Year	Domain	Trait	P-value	N	EA	NEA
31427789	2019	Dermatological	Skin colour	1.87E-05	381433	C	T
31427789	2019	Nutritional	Coffee intake	5.12E-05	358093	C	T
https://doi.org/10.1101/288626	2019	Neurological	Cingulum (hippocampus) mode of anisotropy	8.44E-05	17706	T	C
30573740	2018	Dermatological	Male pattern baldness (BOLT LMM infinitesimal mixed model)	2.30E-04	205327	T	C

Chr 10 rs7894565 Significant P-value 2.94E-04

PMID	Year	Domain	Trait	P-value	N	EA	NEA
doi.org/10.1101/288563	2019	Neurological	Fornix (column and body of fornix) fractiona anisotropy	3.39E-11	17706	C	T
doi.org/10.1101/288651	2019	Neurological	Fornix (column and body of fornix) radial diusivities	1.73E-09	17706	T	C
doi.org/10.1101/288607	2019	Neurological	Fornix (column and body of fornix) mean diusivities	2.64E-09	17706	T	C
doi.org/10.1101/288590	2019	Neurological	Posterior limb of internal capsule axial diusivities	4.87E-09	17706	T	C
30664634	2019	Metabolic	Arms-arm fat ratio (female)	6.54E-09	195068	C	T
doi.org/10.1101/288638	2019	Neurological	Superior corona radiata mode of anisotropy	8.22E-09	17706	T	C
doi.org/10.1101/288585	2019	Neurological	Fornix (column and body of fornix) axial diusivities	2.72E-08	17706	T	C
30531941	2018	Activities	Overall activity	7.30E-08	91105	T	C
doi.org/10.1101/288634	2019	Neurological	Posterior limb of internal capsule mode of anisotropy	1.26E-07	17706	T	C
27863252	2016	Immunological	Monocyte count (three-way meta)	3.66E-07	170721	C	T
27863252	2016	Immunological	Monocyte percentage of white cells (three-way meta)	4.41E-07	170494	C	T
30108127	2018	Metabolic	Body Mass Index	6.90E-07	334487	C	T
31676860	2019	Neurological	Left accumbens area	8.04E-07	19629	C	T
31676860	2019	Neurological	Left accumbens area	1.17E-06	21821	C	T
27863252	2016	Immunological	Granulocyte percentage of myeloid white cells (three-way meta)	1.68E-06	169545	T	C
31676860	2019	Neurological	Total brain volume	1.84E-06	21821	T	C
31676860	2019	Neurological	Total brain volume	2.10E-06	19629	T	C
doi.org/10.1101/288572	2019	Neurological	Superior corona radiata fractional anisotropy	2.93E-06	17706	T	C
27863252	2016	Immunological	Monocyte percentage of white cells (two-way meta)	3.67E-06	131305	C	T
doi.org/10.1101/288568	2019	Neurological	Posterior limb of internal capsule fractional anisotropy	4.15E-06	17706	T	C

doi.org/10.1101/288633	2019	Neurological	Posterior corona radiata mode of anisotropy	4.37E-06	17706	T	C
27863252	2016	Immunological	Monocyte count (two-way meta)	5.17E-06	131544	C	T
doi.org/10.1101/288594	2019	Neurological	Superior corona radiata axial diusivities	6.06E-06	17706	T	C
27863252	2016	Immunological	Granulocyte percentage of myeloid white cells (two-way meta)	1.24E-05	130543	T	C
doi.org/10.1101/288622	2019	Neurological	Anterior limb of internal capsule mode of anisotropy	1.36E-05	17706	T	C
31676860	2019	Neurological	3rd ventricle	1.53E-05	19629	T	C
27046643	2016	Environment	Educational attainment	1.79E-05	111114	T	C
doi.org/10.1101/288629	2019	Neurological	Fornix (column and body of fornix) mode of anisotropy	1.80E-05	17706	C	T
31676860	2019	Neurological	Left lateral ventricle	2.05E-05	19629	T	C
31676860	2019	Neurological	3rd ventricle	2.80E-05	21821	T	C

Chr17 Significant P-value 8.98E-05 rs7221651

PMID	Year	Domain	Trait	P-value	N	EA	NEA
31427789	2019	Metabolic	Impedance measures - Trunk fat mass	7.05E-30	379578	C	T
31427789	2019	Metabolic	Impedance measures - Trunk fat percentage	4.63E-27	379600	C	T
31427789	2019	Metabolic	Impedance measures - Whole body fat mass	8.14E-26	379203	C	T
31427789	2019	Metabolic	Impedance measures - Body fat percentage	1.23E-25	379615	C	T
31427789	2019	Metabolic	Weight	5.56E-23	385473	C	T
31427789	2019	Metabolic	Impedance measures - Weight	7.11E-23	379840	C	T
31427789	2019	Metabolic	Waist circumference	9.77E-22	385932	C	T
31427789	2019	Metabolic	Impedance measures - Arm fat percentage (left)	9.01E-20	379699	C	T
31427789	2019	Metabolic	Impedance measures - Leg fat mass (right)	1.23E-19	379802	C	T
31427789	2019	Metabolic	Impedance measures - Leg fat mass (left)	1.44E-19	379783	C	T
31427789	2019	Metabolic	Impedance measures - Leg fat percentage (left)	1.45E-19	379786	C	T
31427789	2019	Metabolic	Impedance measures - Leg fat percentage (right)	1.27E-18	379806	C	T
31427789	2019	Metabolic	Impedance measures - Arm fat percentage (right)	1.41E-18	379752	C	T
31427789	2019	Metabolic	Impedance measures - Arm fat mass (right)	2.55E-18	379725	C	T
31427789	2019	Metabolic	Impedance measures - Arm fat mass (left)	1.82E-17	379663	C	T
27863252	2016	Immunological	Eosinophil count (three-way meta)	2.22E-17	172275	C	T
31427789	2019	Metabolic	Hip circumference	9.33E-17	385887	C	T
27863252	2016	Immunological	Eosinophil percentage of white cells (three-way meta)	1.66E-16	172378	C	T
27863252	2016	Immunological	Sum eosinophil basophil count (three-way meta)	4.05E-16	171771	C	T
27863252	2016	Immunological	Eosinophil count (two-way meta)	1.70E-15	131999	C	T
27863252	2016	Immunological	Eosinophil percentage of granulocytes (three-way meta)	1.77E-15	170536	C	T
27863252	2016	Immunological	Eosinophil percentage of white cells (two-way meta)	1.77E-15	132052	C	T
27863252	2016	Immunological	Sum eosinophil basophil count (two-way meta)	2.12E-14	131557	C	T
27863252	2016	Immunological	Eosinophil percentage of granulocytes (two-way meta)	3.08E-14	131525	C	T
31427789	2019	Metabolic	Impedance measures - Basal metabolic rate	4.54E-14	379821	C	T
27863252	2016	Immunological	Neutrophil percentage of granulocytes (three-way meta)	8.86E-14	170672	T	C
31427789	2019	Metabolic	Impedance measures - Leg fat-free mass (left)	1.30E-13	379766	C	T
31427789	2019	Metabolic	Impedance measures - Leg predicted mass (left)	1.70E-13	379761	C	T
31427789	2019	Metabolic	Impedance measures - Body Mass Index (BMI)	2.61E-13	379831	C	T
30239722	2018	Metabolic	Body Mass Index	5.19E-13	806834	C	T
31427789	2019	Metabolic	Body Mass Index	5.46E-13	385336	C	T
30664634	2019	Metabolic	Legs-leg fat ratio (female)	6.07E-13	195068	T	C
27863252	2016	Immunological	Neutrophil percentage of granulocytes (two-way meta)	9.21E-13	131660	T	C
31427789	2019	Skeletal	Standing height	1.16E-12	385748	C	T
31427789	2019	Metabolic	Impedance measures - Leg predicted mass (right)	2.65E-12	379793	C	T
31427789	2019	Metabolic	Impedance measures - Leg fat-free mass (right)	2.78E-12	379793	C	T
30239722	2018	Metabolic	Waist-hip ratio	4.06E-12	697734	C	T

doi.org/10.1101/261081	2018	Reproduction	Number of sexual partners	1.14E-11	370711	C	T
31427789	2019	Metabolic	Impedance measures - Arm predicted mass (right)	2.43E-11	379716	C	T
31427789	2019	Metabolic	Impedance measures - Arm fat-free mass (right)	3.33E-11	379723	C	T
31427789	2019	Metabolic	Impedance measures - Whole body water mass	3.49E-11	379835	C	T
31427789	2019	Metabolic	Impedance measures - Whole body fat-free mass	4.56E-11	379804	C	T
30297969	2018	Endocrine	Type 2 Diabetes	1.50E-10	898130	C	T
31427789	2019	Metabolic	Impedance measures - Arm predicted mass (left)	2.78E-10	379638	C	T
31427789	2019	Metabolic	Impedance measures - Arm fat-free mass (left)	5.54E-10	379653	C	T
29970889	2018	Psychiatric	Loneliness (MTAG)	6.20E-09	487647	C	T
31427789	2019	Nutritional	Major dietary changes in the last 5 years	8.65E-09	385587	C	T
30239722	2018	Metabolic	Body Mass Index (female)	2.52E-08	434794	C	T
30664634	2019	Metabolic	Trunk-trunk fat ratio (female)	2.67E-08	195068	C	T
30804560	2019	Respiratory	FEV1/FVC ratio	2.71E-08	400102	C	T
30239722	2018	Metabolic	Waist-hip ratio (female)	3.00E-08	381152	C	T
28892062	2017	Metabolic	Body Mass Index	3.07E-08	158284	T	C
31427789	2019	Metabolic	Impedance measures - Trunk fat-free mass	3.40E-08	379507	C	T
30804560	2019	Respiratory	FEV1/FVC ratio	4.10E-08	321047	C	T
29970889	2018	Psychiatric	Loneliness	5.30E-08	445024	C	T
31427789	2019	Metabolic	Impedance measures - Trunk predicted mass	7.32E-08	379469	C	T
doi.org/10.1101/288628	2019	Neurological	External capsule mode of anisotropy	7.95E-08	17706	C	T
doi.org/10.1101/288632	2019	Neurological	Inferior fronto-occipital fasciculus mode of anisotropy	1.22E-07	17706	C	T
29403010	2018	Metabolic	Alanine aminotransferase	1.97E-07	134182	C	T
doi.org/10.1101/288618	2019	Neurological	Superior longitudinal fasciculus mean diusivities	3.26E-07	17706	C	T
doi.org/10.1101/288611	2019	Neurological	Posterior corona radiata mean diusivities	7.04E-07	17706	C	T
31427789	2019	Skeletal	Comparative height size at age 10	8.22E-07	380167	C	T
doi.org/10.1101/288662	2019	Neurological	Superior longitudinal fasciculus radial diusivities	8.63E-07	17706	C	T
doi.org/10.1101/261081	2018	Activities	First PC of the four riskly behaviours	9.02E-07	315894	C	T
31427789	2019	Activities	Overall health rating	1.01E-06	384850	T	C
31427789	2019	Nutritional	Never eat eggs, dairy, wheat, sugar: I eat all of the above	1.22E-06	384986	T	C
31676860	2019	Neurological	Left caudal anterior cingulate	1.24E-06	21821	T	C
31676860	2019	Neurological	Left caudal anterior cingulate	1.97E-06	19629	T	C
doi.org/10.1101/288601	2019	Neurological	Average across all tracts mean diusivities	2.02E-06	17706	C	T
29403010	2018	Metabolic	Triglyceride	2.09E-06	105597	C	T
28892062	2017	Metabolic	Body Mass Index (male)	2.20E-06	85894	T	C
30239722	2018	Metabolic	Body Mass Index (male)	2.24E-06	374756	C	T

31427789 doi.org/10.11	2019	Social Interactions	Frequency of friend/family visits	2.81E-06	383941	T	C
01/288555 doi.org/10.11	2019	Neurological	Anterior corona radiata fractional anisotropy	3.02E-06	17706	T	C
01/288643	2019	Neurological	Anterior corona radiata radial diusivities	3.59E-06	17706	C	T
30108127	2018	Metabolic	Body Mass Index	3.70E-06	334487	C	T
31427789	2019	Skeletal	Sitting height	4.05E-06	385393	C	T
31427789 doi.org/10.11	2019	Psychiatric	Frequency of tiredness / lethargy in last 2 weeks	4.26E-06	375053	C	T
01/288645	2019	Neurological	Average across all tracts radial diusivities	4.49E-06	17706	C	T
30531953 doi.org/10.11	2018	Neurological	Epilepsy	4.56E-06	44889	C	T
01/288599	2019	Neurological	Anterior corona radiata mean diusivities	4.68E-06	17706	C	T
30598549	2018	Body Structures	Fractures	5.00E-06	426795	C	T
29403010	2018	Metabolic	Gamma-glutamyl transferase	6.04E-06	118309	C	T
29970889 doi.org/10.11	2018	Social Interactions	Social support - Leisure/social activities: Religious group	6.60E-06	452302	T	C
01/288574 doi.org/10.11	2019	Neurological	Superior longitudinal fasciculus fractional anisotropy	9.11E-06	17706	T	C
01/288655	2019	Neurological	Posterior corona radiata radial diusivities	9.88E-06	17706	C	T
31427789	2019	Activities	Number of treatments/medications taken	1.23E-05	386581	C	T
30054458	2018	Endocrine	Type 2 Diabetes	1.65E-05	659256	C	T
31427789 doi.org/10.11	2019	Reproduction	Age first had sexual intercourse	1.90E-05	339614	T	C
01/288584 doi.org/10.11	2019	Neurological	External capsule axial diusivities	2.05E-05	17706	C	T
01/288579	2019	Neurological	Average across all tracts axial diusivities	2.19E-05	17706	C	T
30048462 doi.org/10.11	2018	Skeletal	Heel bone mineral density	2.50E-05	394929	T	C
01/288658	2019	Neurological	Retrolenticular part of internal capsule radial diusivities	2.78E-05	17706	C	T
31427789	2019	Psychiatric	Loneliness, isolation	3.02E-05	380317	C	T
31427789	2019	Activities	Health satisfaction	3.07E-05	128745	T	C
31676860	2019	Neurological	White matter	3.54E-05	21821	C	T
31427789 doi.org/10.11	2019	Nutritional	Never eat eggs, dairy, wheat, sugar: Sugar or foods/drinks containing sugar	3.62E-05	384986	C	T
01/288557	2019	Neurological	Average across all tracts fractional anisotropy	3.91E-05	17706	T	C
29500382	2018	Psychiatric	Loneliness, isolation (LONE)	4.60E-05	267190	C	T
31427789 /10.1101/288	2019	Activities	Types of physical activity in last 4 weeks: Light DIY (eg: pruning, watering the lawn)	4.62E-05	384450	T	C
613	2019	Neurological	Posterior thalamic radiation (include optic radiation) mean diusivities	5.12E-05	17706	C	T
31427789 doi.org/10.11	2019	Body Structures	Fractured/broken bones in last 5 years	5.56E-05	384446	C	T
01/288657	2019	Neurological	Posterior thalamic radiation (include optic radiation) radial diusivities	5.84E-05	17706	C	T

doi.org/10.11 01/288614	2019	Neurological	Retrolenticular part of internal capsule mean diusivities	6.06E-05	17706	C	T
doi.org/10.11 01/288660	2019	Neurological	Superior corona radiata radial diusivities	6.76E-05	17706	C	T
31676860	2019	Neurological	White matter	7.26E-05	19629	C	T
31427789	2019	Activities	Medication for cholesterol, blood pressure, diabetes, or take exogenous hormones: Cholesterol lowering medication	7.47E-05	207533	C	T

Chr19	Significant P-value 5.1E-04			rs612285			
PMID	**Year**	**Domain**	**Trait**	**P-value**	**N**	**EA**	**NEA**
30804566	2019	Neurological	Frequent insomnia symptoms	1.40E-04	237627	A	G
31427789	2019	Reproduction	Age at menopause (last menstrual period) (female)	2.89E-04	119160	A	G
31427789	2019	Reproduction	Had menopause (female)	3.35E-04	175519	G	A

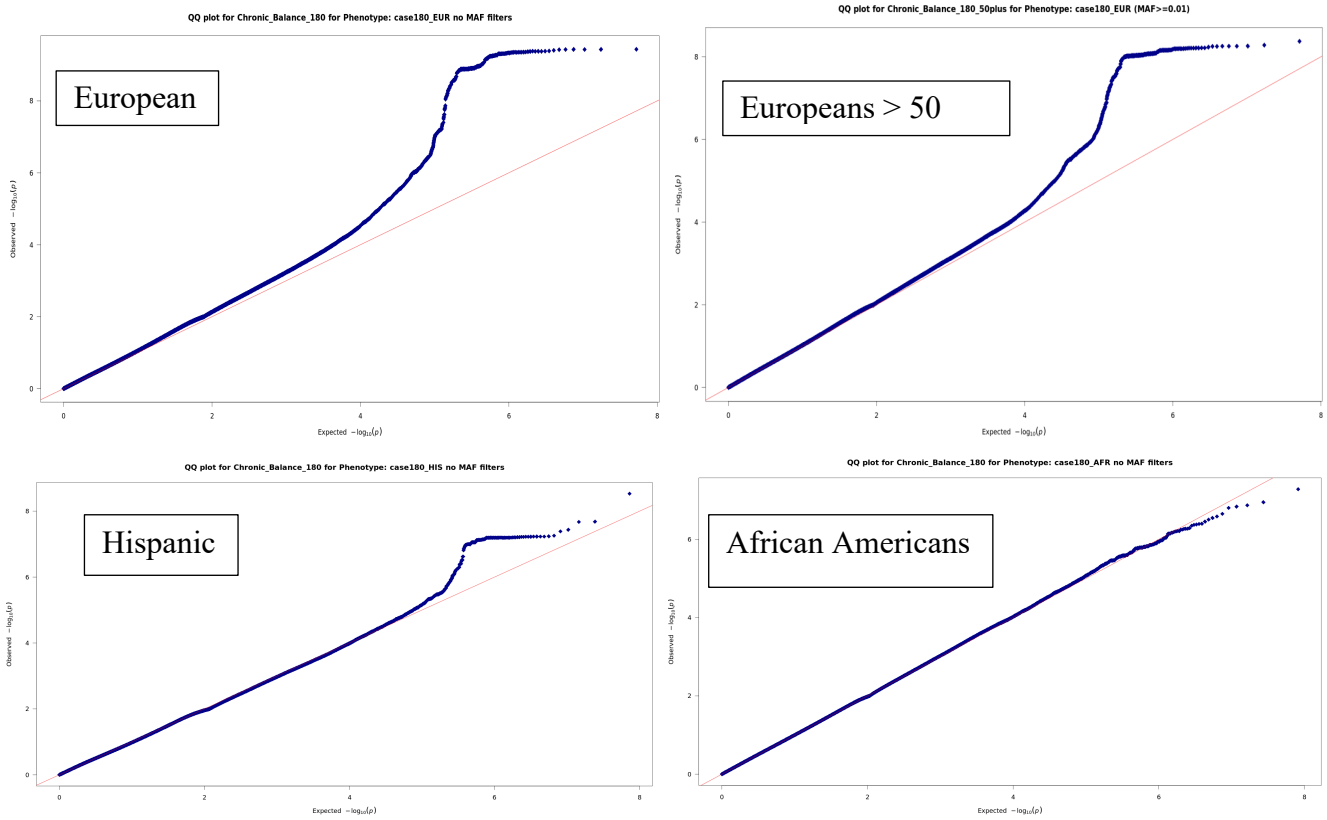

Figure e1: Quantile-quantile plot of expected versus observed -log10 *P*-values for a genome-wide association study (GWAS) of balance.

A. QQ-Plot European. **B.** QQ-Plot Europeans > 50 years of age**.** **C.** QQ-Plot Hispanic Ancestry.

D. QQ-Plot African American Ancestry. Quantile-quantile plots show the distribution of expected versus observed *P* Values for the GWAS in the Million Veteran Program cohort consisting of 50,339 cases of chronic imbalance and 366,900 controls. Filtering was performed to include only SNPs with P-value < 1 x 10^{-05}; For the European analysis, GC ƛ = 1.127; LDSC intercept ($h_{2\ int}$ = 1.027, SE = 0.0079). Polygenic effects account for 94.8% of the observed inflation.

Figures e2 through e9. Chromosome base positions are aligned on each figure.

A. Chromosomal position is indicated on the x-axis. -log10 *P*-values for each single nucleotide polymorphism (SNP) (filled circles) are indicated on the y-axis, with the lead SNP shown in purple. Annotated genes in the region are drawn in the lower panel. Recombination rate is indicated by a blue line. Additional SNPs in the locus are colored according to linkage disequilibrium (r^2) with the lead SNP. Recombination rates estimated from the CEU HapMap population represented by the vertical blue line.

B. Combined Annotated Dependent Depletion (CADD) scores for top, lead, and independent significant SNPs. CADD is an *in silico* prediction of variant pathogenicity. Scaled CADD score of 10 indicates that the variant is among the top 10% of deleterious variants.

C. RegulomeDb is a database with annotations of regulatory elements, i.e., transcription factor binding, transcription factor motifs, Dnase peaks and eQTLs. Lower numbers (1a-f) indicate a higher chance of a regulatory b binding site SNP. 7 indicates no binding site noted.

D. Chromatin state in the region of significant hits.

E. Where noted, eQTLs for genes within the locus, different colors represent different tissues that are indicated on the right side of the diagram. Significance is at FDR < .05.

F. Where noted, Hi-C results indicate intrachromatin capture (eFigure 9 only).

Figure e2. Regional association plot (Locus zoom) top hit rs12779865 in trans-ancestry analysis.

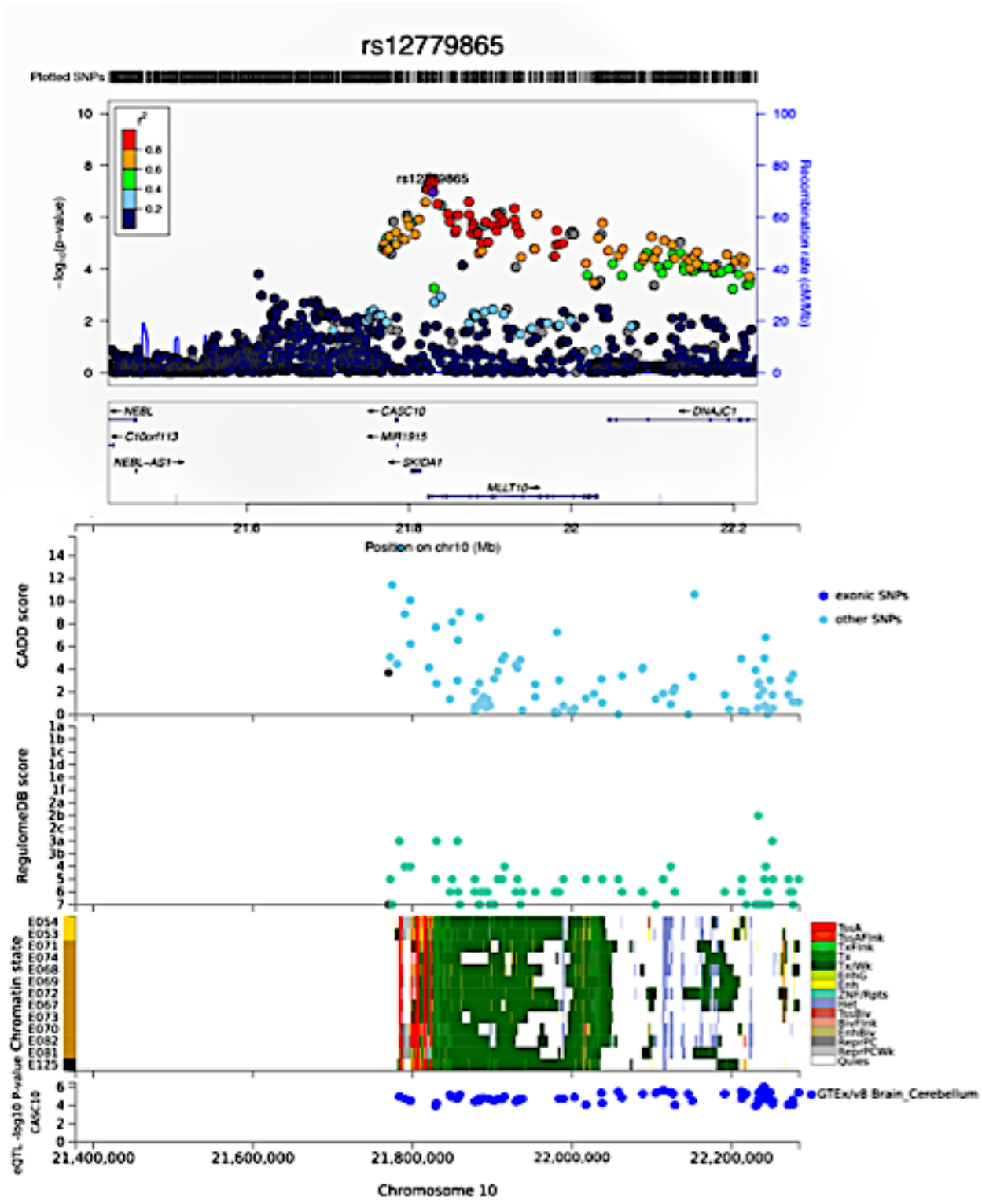

Figure e3. Regional association plot (Locus zoom) top hit rs72631329 in trans-ancestry analysis.

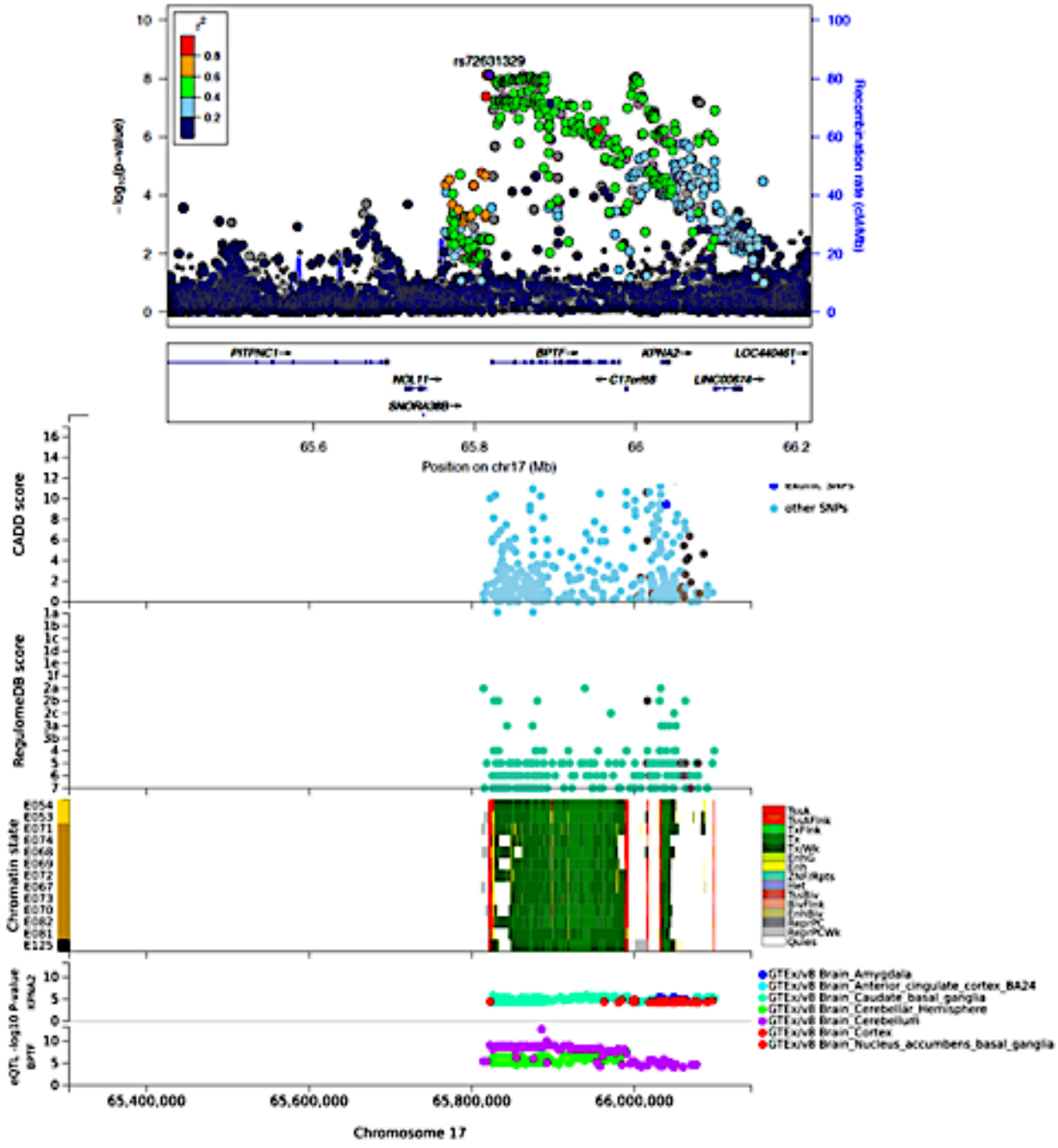

Figure e4. Regional association plots (Locus zoom) top hit rs10713223 in trans-ancestry analysis.

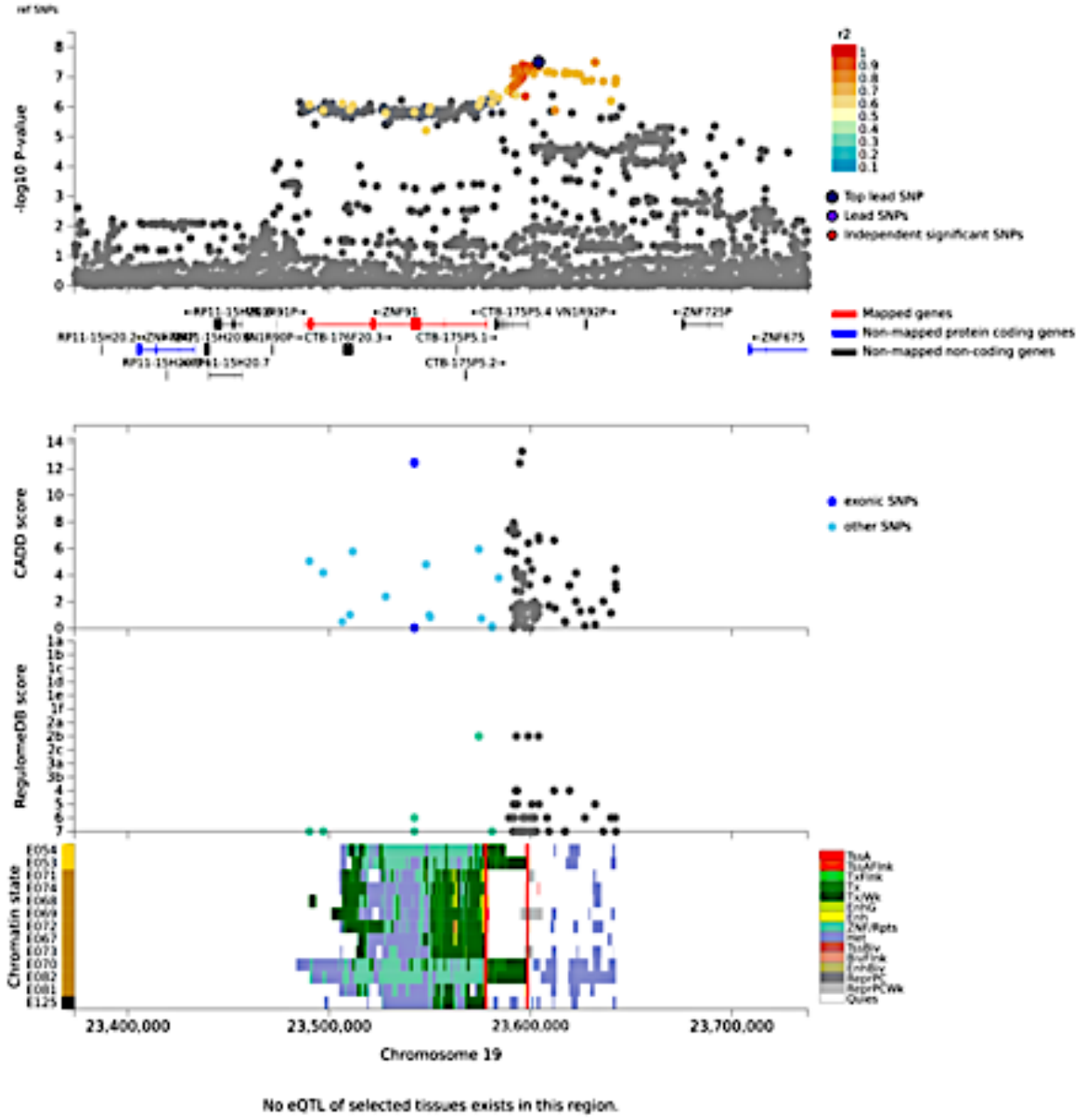

No eQTL of selected tissues exists in this region.

Figure e5. Regional association plots (Locus zoom) of top hit rs200689072 in transancestry GWAS.

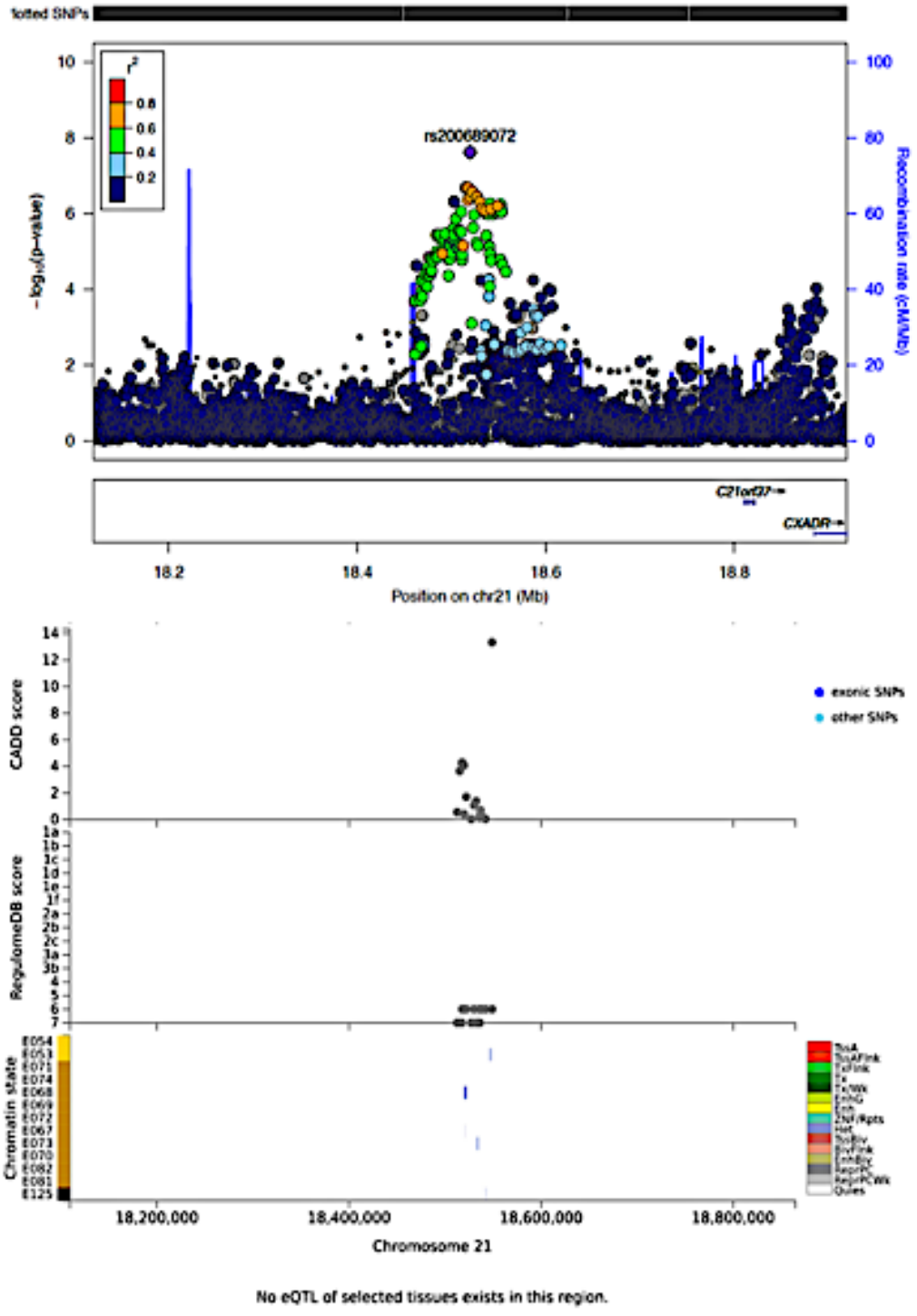

eFigure 6. Regional association plots (Locus zoom) of top hit rs10828248 in European analysis.

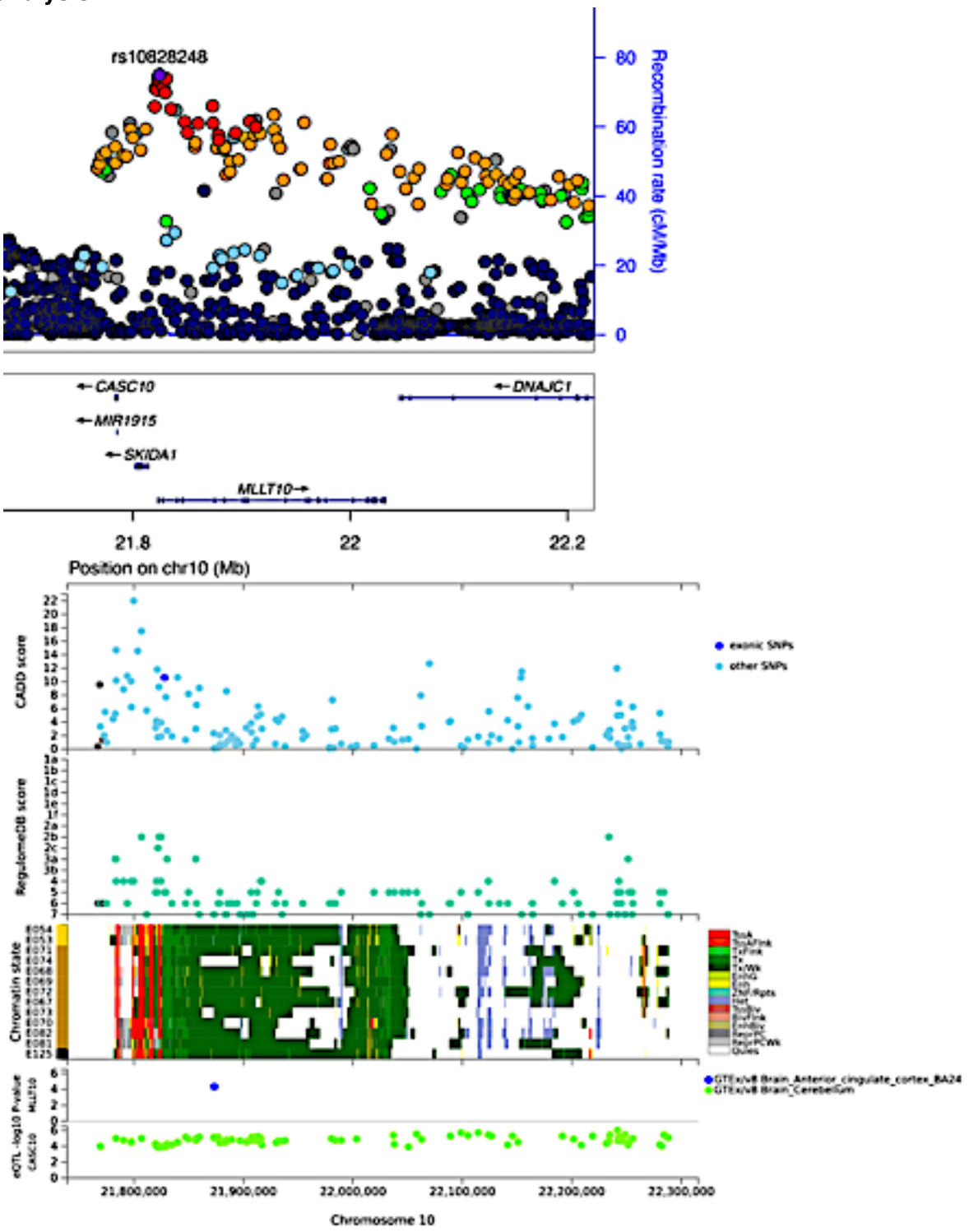

eFigure 7. Regional association plots (Locus zoom) of top hit rs7221651 in European analysis.

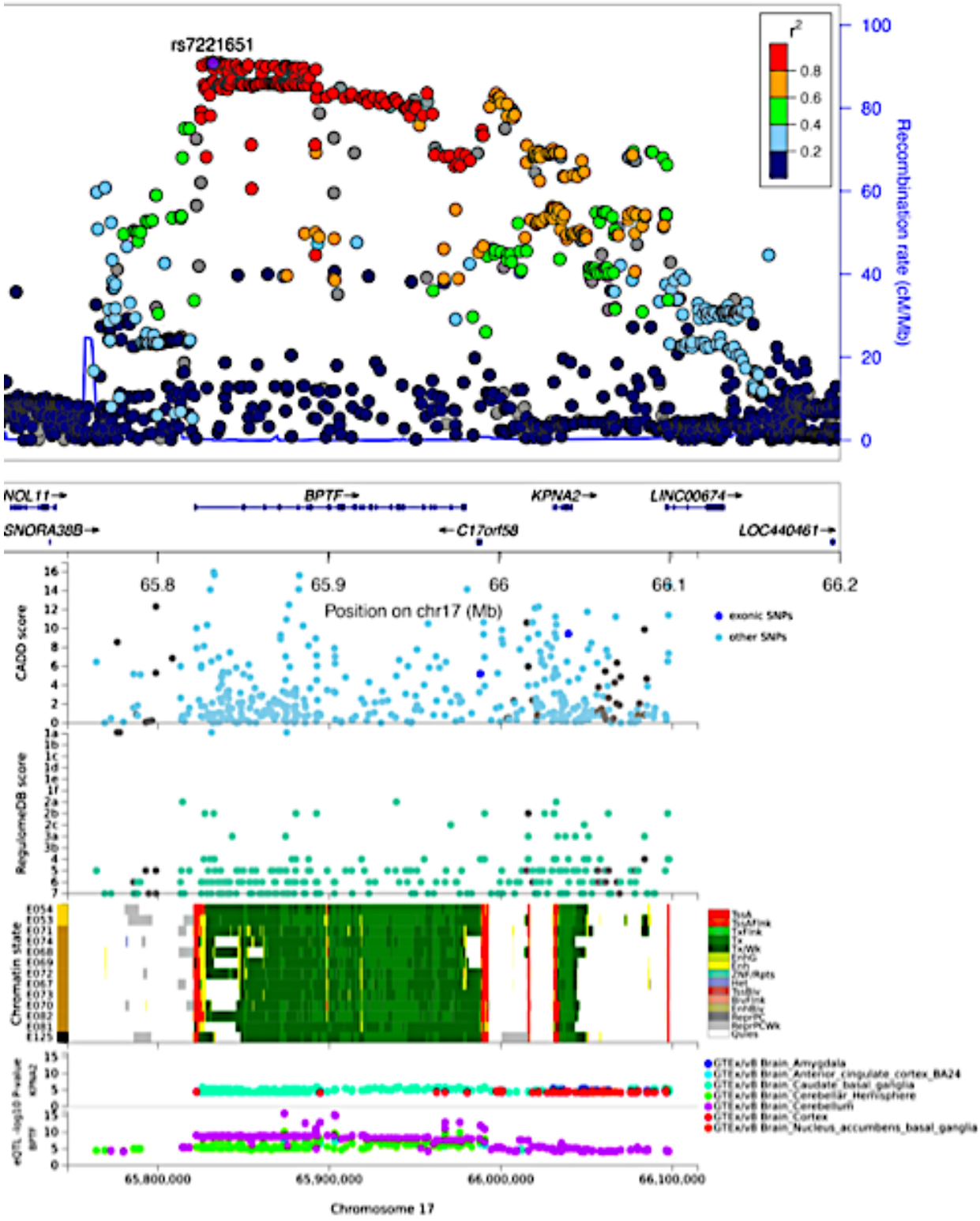

eFigure 8. Regional association plots (Locus zoom) of top hit rs4791046 in Europeans over the age of 50.

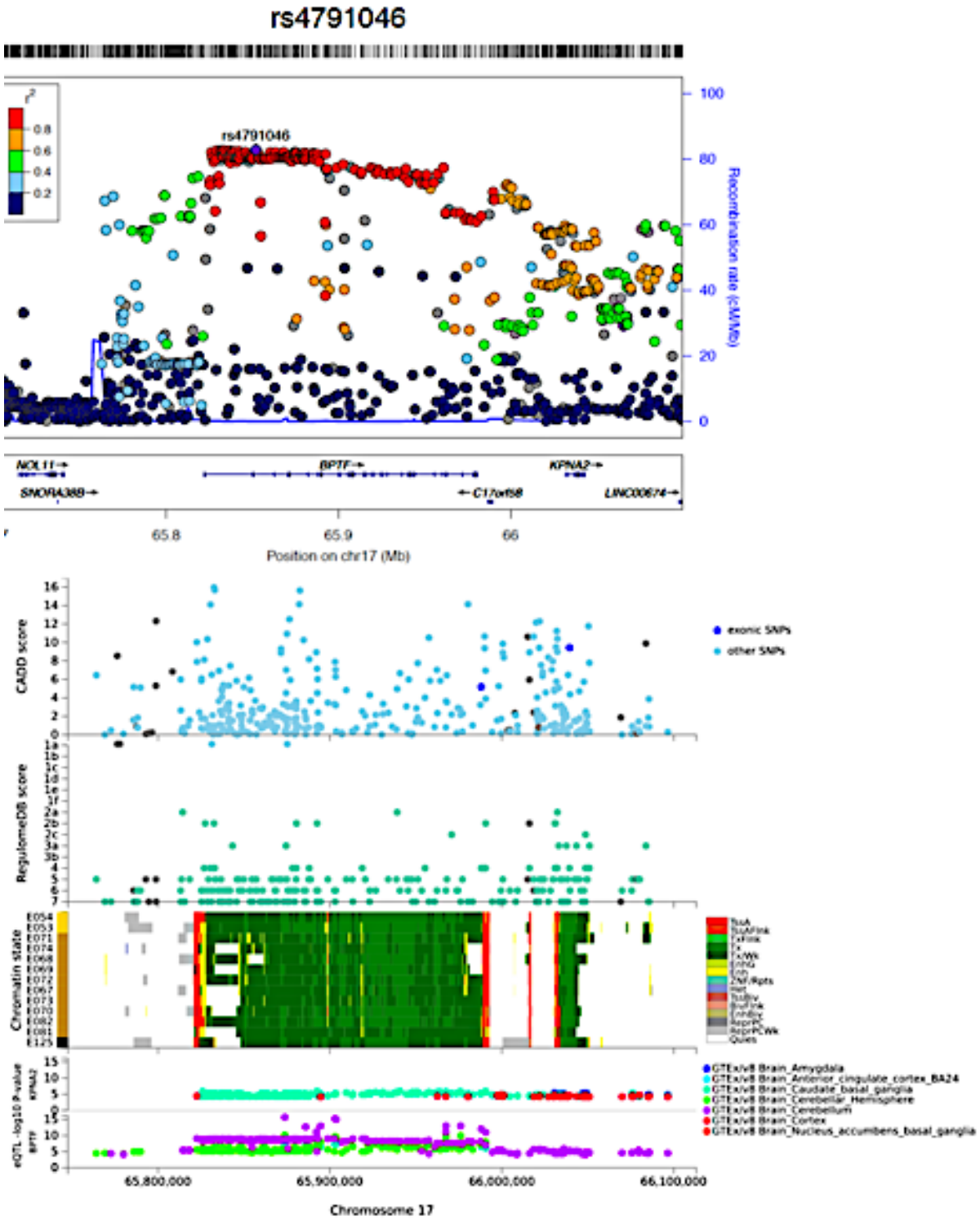

eFigure 9. Regional plot of top hit rs71717606 in Hispanic ancestry GWAS.

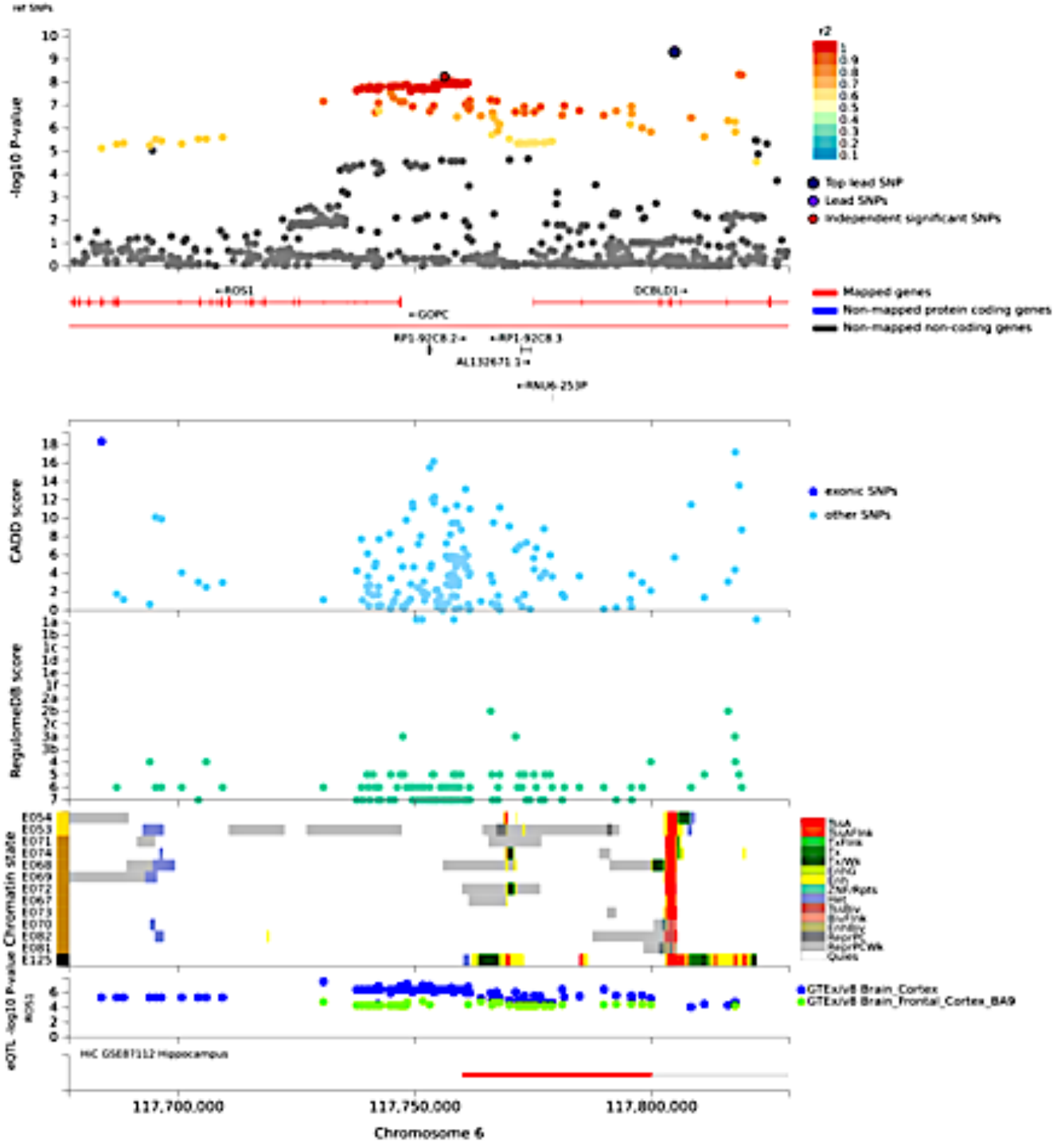

eFigure 10. Fine Mapping Plots

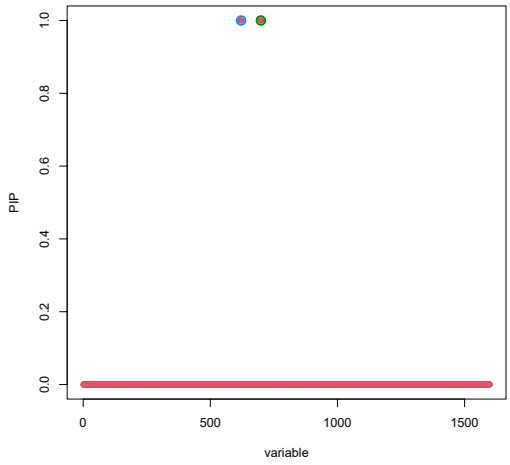

a. Chromosome 6 – MXL ancestry

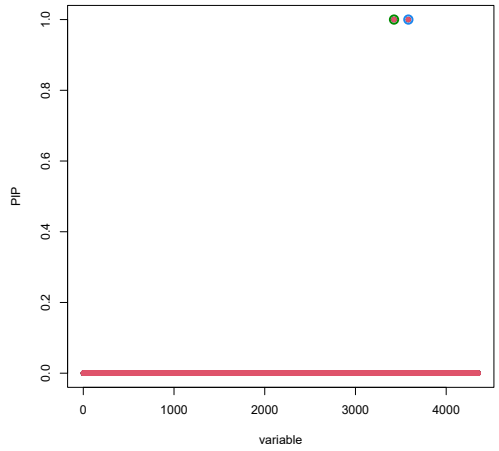

b. Chromosome 10 – CEU ancestry

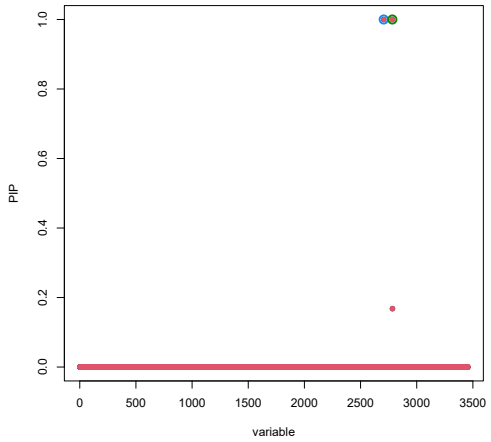

c. Chromosome 17 – CEU ancestry

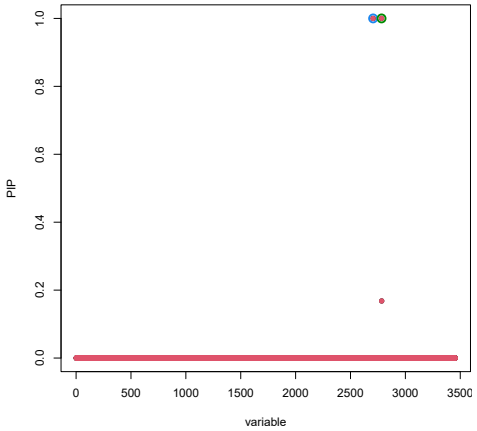

d. Chromosome 19 – CEU, MXL, ASW

Notes: the red dots indicate SNPs that are part of credible sets. PIP indicates posterior inclusion probability of potential causal variants.

Figure e11. PheWAS on lead SNPs

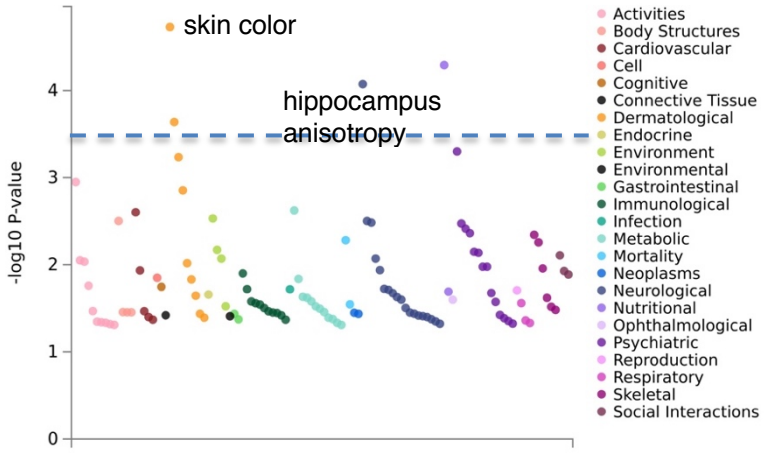

Figure e11a. PheWAS chr6 - rs72965321 - on 3,300 traits. See Table e5 for numeric values. Dotted line indicates significant P-value < 2.94E-04.

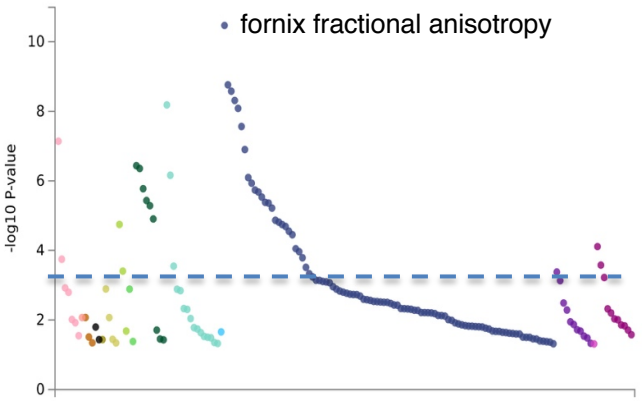

Figure e11c. PheWAS chr10 - rs7894565 - on 3,300 traits. See Table e5 for numeric values. Dotted line indicates significant P-value < 4.31E-04.

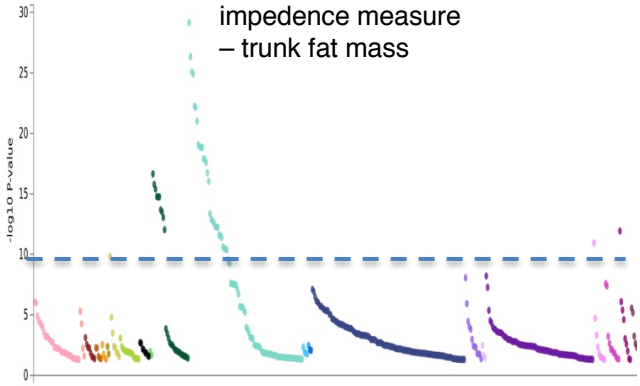

Figure e11c. PheWAS chr17 - rs7221651 - on 3,300 traits. See Table e5 for numeric values. Dotted line indicates significant P-value < 8.98E-05.

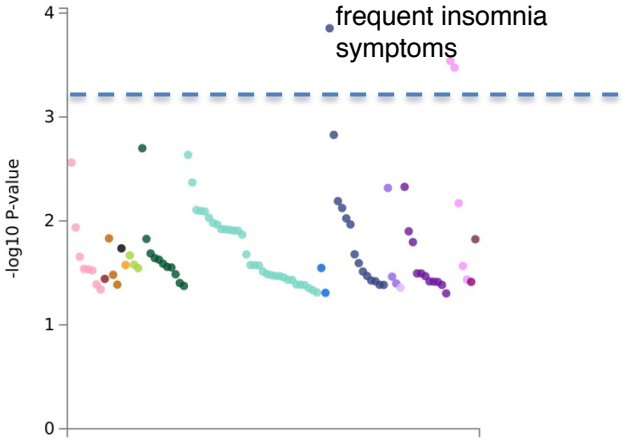

Figure e11d. PheWAS chr19 - rs612285 - on 3,300 traits. See Table e5 for numeric values. Dotted line indicates significant P-value < 5.10E-04.